Ultramicroscopy 110 (2010) 612–617

Contents lists available at ScienceDirect

Ultramicroscopy

journal homepage: www.elsevier.com/locate/ultramic

Step response measurement of AFM cantilever for analysis of frequency-resolved viscoelasticity

Tatsuya Ogawa, Shinkichi Kurachi, Masami Kageshima *, Yoshitaka Naitoh, Yan Jun Li, Yasuhiro Sugawara

Department of Applied Physics, Graduate School of Engineering, Osaka University, 2-1 Yamada-oka, Suita, Osaka 565-0871, Japan

ARTICLE INFO

Keywords:
Atomic force microscopy
Soft matter
Viscoelasticity
Water
Step response
Magnetic force

ABSTRACT

Extension of AFM-based viscoelasticity measurement into a frequency-resolved analysis is attempted. A cantilever immersed into and interacting with distilled water was employed for the trial system. Using a home-built wideband magnetic excitation AFM, a step force with a transient time less than 1 μs is applied to the AFM cantilever and its deflection is measured. The 1st and 2nd mode resonance ringing of the cantilever was suppressed using quality-factor-control technique, so that the measurement system becomes equivalent to driving a resonance-free virtual cantilever within the bandwidth limited by the surviving 3rd mode resonance. From the obtained response of the cantilever deflection, a frequency-dependent complex compliance of the cantilever-water system was derived in a frequency range of 1–100 kHz. Effect of water confining between the tip and a mica substrate is discussed.

1. Introduction

A viscoelasticity, defined as a complex transfer function of a system's deformation with respect to an applied force, is a relevant quantity in understanding its dynamical properties. It has been a long tradition in the research of soft-matter systems like polymers, liquid crystals, fluids, etc. to measure their viscoelastic responses. It should be stressed that a combination of elastic and viscous properties of a system determines one time scale. In the most simplified picture this is understood as the time required for an object bound with an elastic bond and displaced from its equilibrium position to return there against a viscous drag force, i.e., a relaxation time. However, in general, a soft-matter has a number of elastic and viscous components, resulting in hierarchical time scales dispersed over orders of magnitude. In order to resolve this hierarchy it has been a convention to measure the viscoelasticity of the system under study in a form of frequency-resolved spectrum.

The atomic force microscopy (AFM) proved to be a powerful tool for also analyzing mechanical properties of an extremely localized area. It was also demonstrated that the AFM can be used as a tool for measuring their characteristic interaction force of a single pair of macromolecules [1,2] or stretching force of a single macromolecule [3]. This approach was later combined with the dynamic-mode AFM measurement utilizing oscillating cantilever and was extended to the viscoelastic measurement of single polymer chains [4–11], confined fluids [12–14], cells [15], etc.

Although resonance oscillation of the cantilever is advantageous in enhancing the force sensitivity, its frequency selectivity imposes a limitation to the frequency-resolved analysis. Consequently measurement of frequency-dependent viscoelasticity using AFM has been scarcely attempted except for those in low or narrow frequency ranges [15,16]. Characteristic time scale of a viscoelastic system often spans over orders of magnitude and can be dispersed beyond 1 MHz especially for a polymer system. Recently the cantilever excitation technique using a magnetic force [17,18], a method compatible for liquid environment relevant to soft-matter systems, was extended to cover a bandwidth of 1 MHz including several resonance modes of a standard cantilever [11]. Although measurement of frequency-dependent viscoelasticity spectrum of a single polymer chain was demonstrated by analyzing each resonance peaks, the measurement still had drawbacks of rather long data acquisition time and discreteness of the frequency. It should be noted that minimizing the acquisition time is especially required for analysis of soft matters so that the measurement can be completed before the probe is significantly displaced by thermal drift that is inevitably pronounced in liquid. In the present article, an alternative approach in time domain measurement utilizing the cantilever's transient response is demonstrated.

For the trial system for the present preliminary measurement, a cantilever immersed in water was chosen. Local dynamical property of water interacting with a hydrophilic surface draws scientific attention since it is relevant to various life phenomena,

* Corresponding author. Tel.: +81 6 6879 7854; fax: +81 6 6879 7856.
E-mail address: kage@ap.eng.osaka-u.ac.jp (M. Kageshima).

0304-3991/$ - see front matter © 2010 Elsevier B.V. All rights reserved.
doi:10.1016/j.ultramic.2010.02.020

especially molecular scale ones. Microscopic properties of liquid solvation on solid surfaces have been studied intensively using AFM [12–14,19–23] or similar local probe techniques [24]. It was reported that a thin water layer confined between hydrophilic surfaces has an anomalously long relaxation time of the order of 10^{-4}–10^{-1} s [12,14]. This is surprising since the relaxation time of bulk water at RT is around 10^{-12} s and even that of ice is still around 10^{-6} s [25]. On the other hand, however, it was suggested based on dielectric relaxation measurement that a water layer of extremely low viscosity exists on an actin filament and dominate the motion of myosin molecules on it [26]. This is contrary to the reported anomalously long relaxation time mentioned above. Thus, local behavior of water on biological surfaces is still controversial and is itself an intriguing research subject.

Discussing various properties, especially viscosity, of fluids from a molecular viewpoint was initiated as early as in 1930s [27,28]. The recent advances in microscopic experimental approaches will provide an opportunity to directly reexamine the theories from the basis. Although the results shown in the present article are on water, same idea and approach is, as described later, considered to be valid in measurement of polymer systems, which is also an intriguing research subject.

2. Theory

The fundamental idea of the step response measurement is versatile and common in dynamical analysis of various mechanical or electrical systems. Here only the principle relevant to the present research is briefly described [29]. Suppose a sinusoidal input signal $X(t)=\mathrm{Re}(\hat{X}e^{i\omega t})$ is provided to the system under study and an output signal $Y(t)=\mathrm{Re}(\hat{Y}e^{i\omega t})$is obtained. Here ω is the angular frequency, t the time, and the hat stands for a complex quantity. The corresponding frequency response function is given as $M(i\omega)=M'(\omega)-iM''(\omega)=\hat{Y}/\hat{X}$, where $M'(\omega)$ and $M''(\omega)$ are the real and imaginary parts, respectively. A frequency domain analysis is to measure $M(i\omega)$ while sweeping the frequency. On the other hand, in a typical and simplest time domain analysis, a pulse input $\delta(t)$ or a step input $s(t)=\begin{cases}0 & (t<0\\ s_0 & (t\geq 0\end{cases}$ is provided to the system, where s_0 is a constant, and the corresponding output signal $m(t)$ or $u(t)$, respectively, is measured. The pulse response $m(t)$ and the step response $u(t)$ are related to each other as

$$u(t)=\int_0^t m(t')dt'. \tag{1}$$

In the present experiment, as explained later, the force applied to the cantilever and the resultant deflection are regarded as the input and the output, respectively. Therefore the corresponding frequency response function is a compliance $J(i\omega)=J'(\omega)-iJ''(\omega)$ of the combined cantilever–sample system, the real and imaginary parts of which can be derived by the Fourier–Laplace transformation of $m(t)$;

$$\begin{pmatrix}J'(\omega)\\ J''(\omega)\end{pmatrix}=\int_0^\infty m(t)\begin{pmatrix}\cos\omega t\\ \sin\omega t\end{pmatrix}dt. \tag{2}$$

Thus, by measuring $u(t)$ of the system and applying Eqs. (1) and (2) to it, the frequency-resolved compliance $J(i\omega)$ can be derived.

3. Experimental

A home-built wideband magnetic excitation system installed into a commercial AFM apparatus was used. A magnetic field is generated by a small electromagnet placed beneath the sample holder of the AFM apparatus. The electromagnet and the circuit to drive it were slightly modified from the ones described in the previous report [11] and are shown in Fig. 1(a). The current in the electromagnet is detected as a voltage drop across a non-inductive resistor and is fed back to a constant-current driving circuit that is a composite amplifier of an OP amp and a wideband high-voltage amplifier. The electromagnet is a coreless solenoid with 10 turns and a diameter of ca. 2 mm, leading to reduction of an inductive load for the driver compared to the previous version, hence extension of the excitation bandwidth to ca. 2 MHz. A spherical magnet of NeFeB typically smaller than 10 μm in diameter was attached onto a commercially available SiN cantilever with a nominal spring constant of 0.03 N/m and was magnetized in a static magnetic field of about 0.4 T overnight. Fig. 1(b) shows a response of the current to a step input signal measured as an output signal of the differential amplifier in Fig. 1(a). It is shown that a current jump of 1 A stabilizes in a transient time of about 500 ns and an additional group delay time of about 100 ns caused by the circuit and the transmission line. Since the generated magnetic field is proportional to the magnitude of the current, the magnetic force exerted onto the cantilever having a permanent magnetic dipole is, whether it originates from magnetic gradient or magnetic torque, considered to be proportional to the current. Thus, it is possible to apply a well-regulated step force to a cantilever with a transient time less than 1 μs.

Fig. 2(a) shows a typical profile of cantilever deflection as a response to a 500 Hz square wave driving signal averaged 128 times and recorded as the cantilever was immersed in distilled water and held more than 0.5 mm apart from the bottom of liquid cell, i.e., completely free of any hydrodynamic squeezing effects. It exhibits a substantial ringing due to its resonance modes. A magnified profile of the transient part (Fig. 2(b)) shows that the ringing is composed of several flexural resonance modes of the cantilever. From the thermal noise profile of a cantilever of the same type measured in distilled water shown in Fig. 2(c),

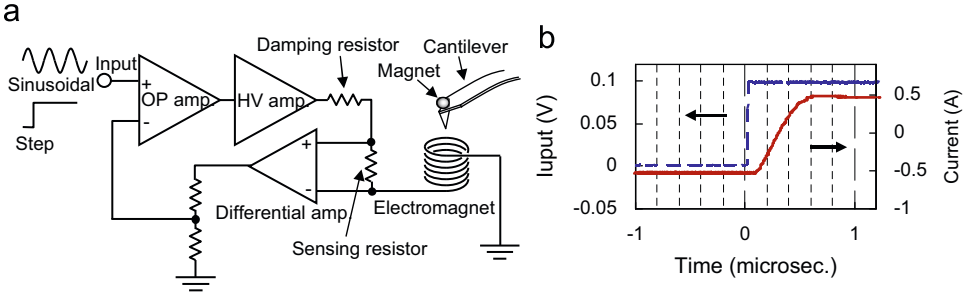

Fig. 1. (a) Schematic diagram of the magnetic excitation system and a cantilever with a spherical magnet. A magnetic force proportional to the input voltage of the drive circuit is applied to the cantilever whether the signal is sinusoidal or step. (b) Response of the current induced in the electromagnet (solid line) to a step input signal (broken line) measured as an output voltage of the differential amplifier in (a).

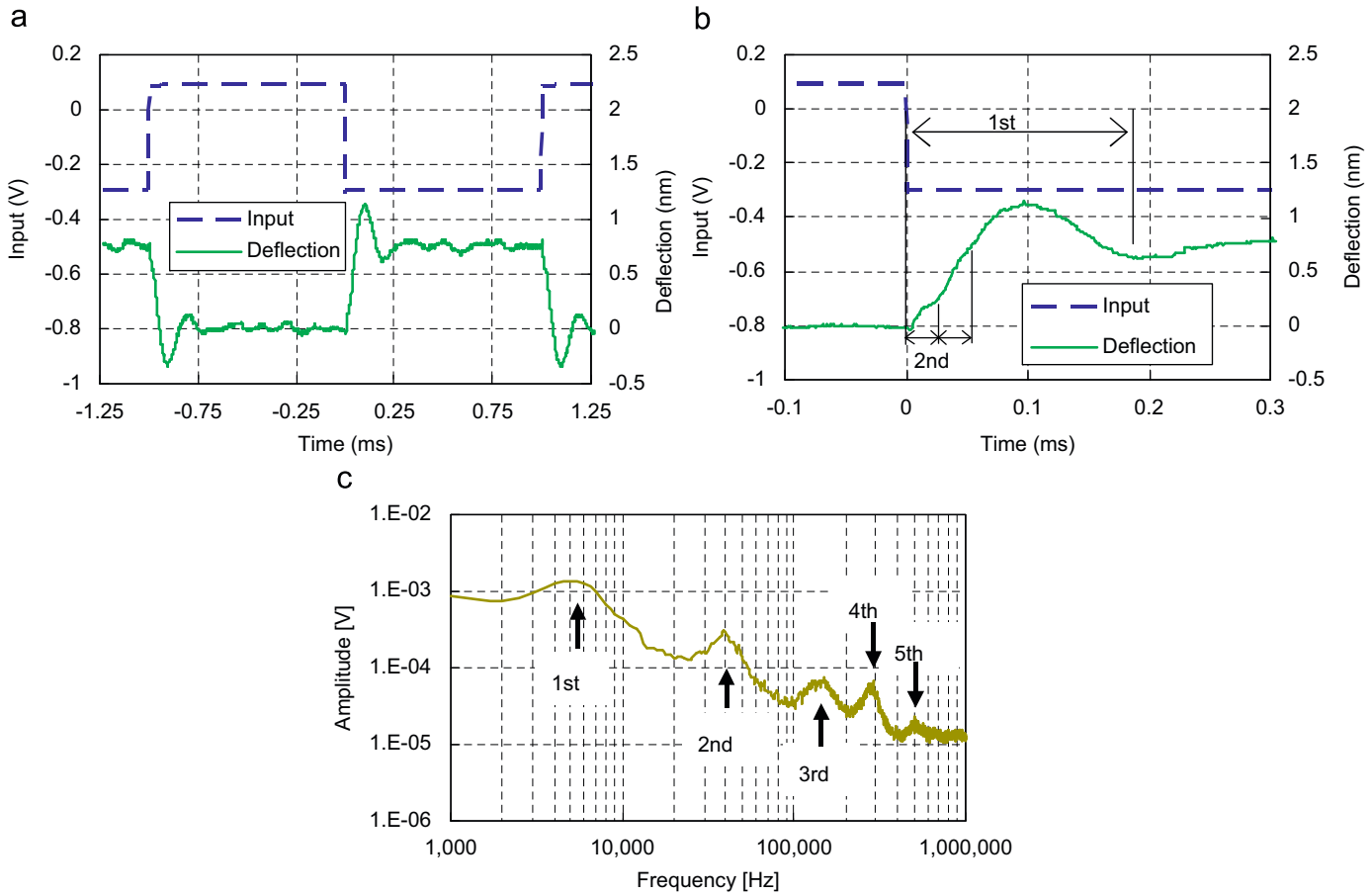

Fig. 2. (a) Typical response in cantilever displacement (solid line) to a 500 Hz square wave input (broken line) measured in distilled water. (b) Magnified transient part of profiles in (a). (c) Typical thermal noise profile of the cantilever measured in water. The 1st–5th resonance modes are shown.

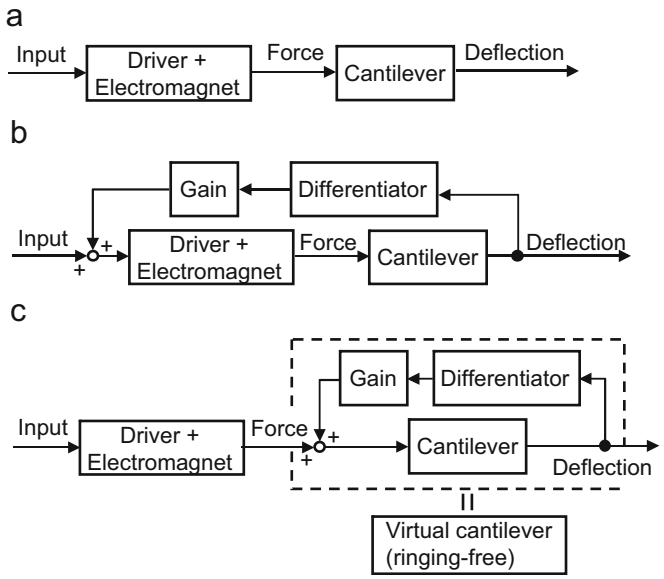

Fig. 3. (a) Schematic diagram of cantilever excitation. (b) Schematic diagram of cantilever excitation with a Q-control loop composed of a differentiator and a gain to suppress the resonance. (c) Equivalent of (b) converted by introducing a gain of different definition.

the major components of this ringing are the 1st and the 2nd modes located at about 6 and 40 kHz, respectively, whereas ringing components due to higher modes are below the noise level which was roughly 1 mV_{p-p} in the frequency band including the 3rd mode and the higher ones. This ringing is a challenge to the transient measurement. Eliminating these resonance modes was attempted using the quality-factor-control (Q-control) technique [30]. The block diagrams of the cantilever response measurement without and with the Q-control loop are shown in Figs. 3(a) and (b), respectively. The Q-control loop consists of a single OP amp differentiator and a gain factor. Since the magnetic force exerted onto the cantilever is proportional to the input voltage of the magnet driver within the present excitation bandwidth, the schematic diagram of the net system can be equivalently rewritten as in Fig. 3(c) by virtually introducing a different gain factor. Comparing Fig. 3(c) with Fig. 3(a), it is shown that the present analysis is same as measuring the response of a virtual cantilever free of resonance ringing. Since a differentiator increases noise, a pole frequency was set at 80 kHz, i.e., between the 2nd and the 3rd resonance modes, so that components higher than this frequency are not differentiated.

4. Results and discussion

Fig. 4 shows waveforms of the electromagnet current and the cantilever deflection measured in distilled water while the Q-control loop was activated to suppress the ringing. Although the 1st and 2nd mode oscillations are well suppressed in the deflection profile in Fig. 4(a), the magnified current and deflection profiles in Fig. 4(b) show that the 3rd mode ringing at about 120 kHz is enhanced instead. This is due to the phase shift caused by the above mentioned 80 kHz pole in the differentiator.

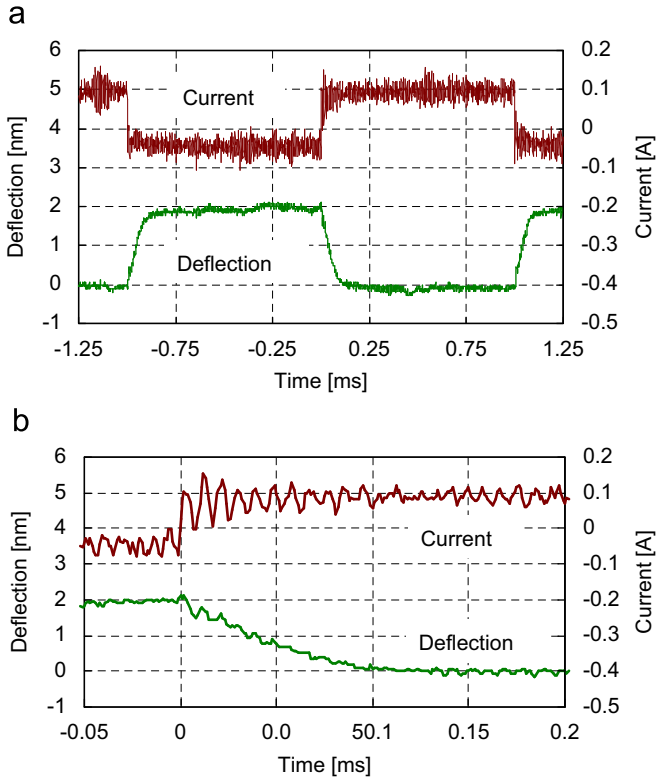

Fig. 4. (a) Profiles of current in the electromagnet (upper) and cantilever deflection (lower) as a response to 500 Hz square wave measured by 128 times averaging while the Q-control loop was activated to suppress 1st and 2nd resonance mode. (b) Magnified transient part of profiles in (a).

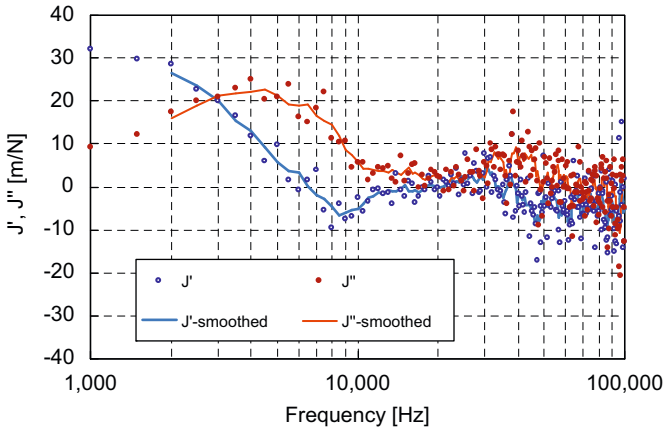

Fig. 5. Frequency-resolved complex compliance of cantilever-water system derived by the Fourier–Laplace transform of the cantilever deflection from 0–1 ms in Fig. 4 (a). Real and imaginary parts are indicated in open and filled figures, respectively. Results of smoothing by taking moving average of 5 data points are also indicated in broad and fine lines for real and imaginary parts, respectively.

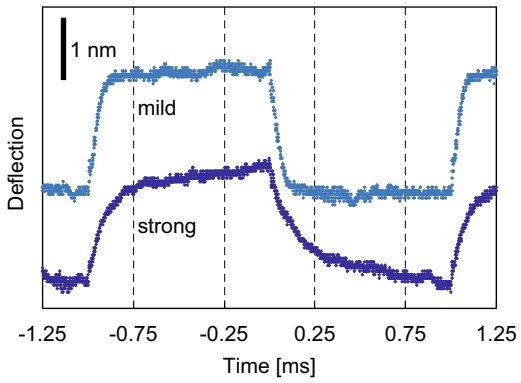

Fig. 6. Profiles of cantilever deflection measured in the same way as in Fig. 4(a) while the tip is apart from a mica substrate by about 600 nm (mild interaction) and about 3 nm (strong interaction).

This ringing gave the frequency upper limit and the analysis was carried out below 100 kHz.

The deflection of the cantilever from 0 to 1 ms in Fig. 4(a) was rescaled to the compliance so that its right-end equaled inverse of cantilever's nominal stiffness 33.3 m/N and was converted to the pulse response function $m(t)$ by numerically differentiating it with time. Complex compliance $J(i\omega)$ was calculated by integrating $m(t)$ over the full duration with a weight of $\sin\omega t$ or $\cos\omega t$ using Eq. (2), where $\omega/2\pi$ was varied from 1 to 100 kHz with an interval of 500 Hz. The result is shown in Fig. 5. Since this data contains a lot of noise especially in the high frequency regime, result of smoothing by moving average is also shown. The most characteristic with this data is the behavior between 1 and 10 kHz. The real part J' exhibits almost the static compliance of the cantilever at the lowest end and decays monotonously to zero with the frequency. The negative J' found around 9 kHz is considered to be an error, and in the higher frequency range J' does not show any significant positive value, at least within the present noise level. On the other hand, the imaginary part J'' shows an increasing trend toward 5 kHz and then decays. Although this frequency coincides with the reported anomalous long relaxation time of water on mica [12], under this condition the cantilever is well apart from any substrate and such a result cannot be expected. In addition, the peak width is too small for a relaxation-type peak that can usually span over orders of magnitude. More probably this is, as well as the dip in J' around 9 kHz, is an influence of 1st resonance mode peak cancelled inappropriately. However, it should be noted that, in contrast to J', it still maintains a significantly positive value up to ca. 50 kHz.

Although the viscoelastic perturbation imposed on the cantilever by water is distributed over the entire cantilever body, as the tip is brought close to a substrate, the local viscoelasticity of water confined between the tip and the substrate like hydrodynamic squeezing and solvation structuring is expected to emerge in the measured compliance. Therefore similar measurements were carried out while bringing the tip cantilever close to a cleaved mica substrate in distilled water. Data obtained under two conditions are compared: when the tip is about 600 nm (mild interaction) and about 3 nm (strong interaction) apart from the substrate. The measured profiles of cantilever deflection under these two conditions are shown in Fig. 6. There is an obvious difference between the two profiles; the settling time becomes substantially longer with the "strong" interaction. Conversion to compliance spectrum was carried out in the same way as used for calculating the data in Fig. 5. Because the cantilever deflection does not reach the stationary state in 1 ms in the "strong" interaction data, the factor for rescaling the "mild" data to 33.3 m/N is applied to the both data. This insufficient pulse duration is considered to affect reliability of the measured compliance in its low frequency part only. The changes in real and imaginary parts of the compliance are shown separately in Fig. 7. For mildly interacting cantilever both J' and J'' exhibit almost same feature as shown in Fig. 5. On the other hand, the strongly interacting cantilever shows a substantial suppression both in J' and J'', although the low J' value at the low frequency end is attributed to the error by insufficient pulse duration mentioned above. In the

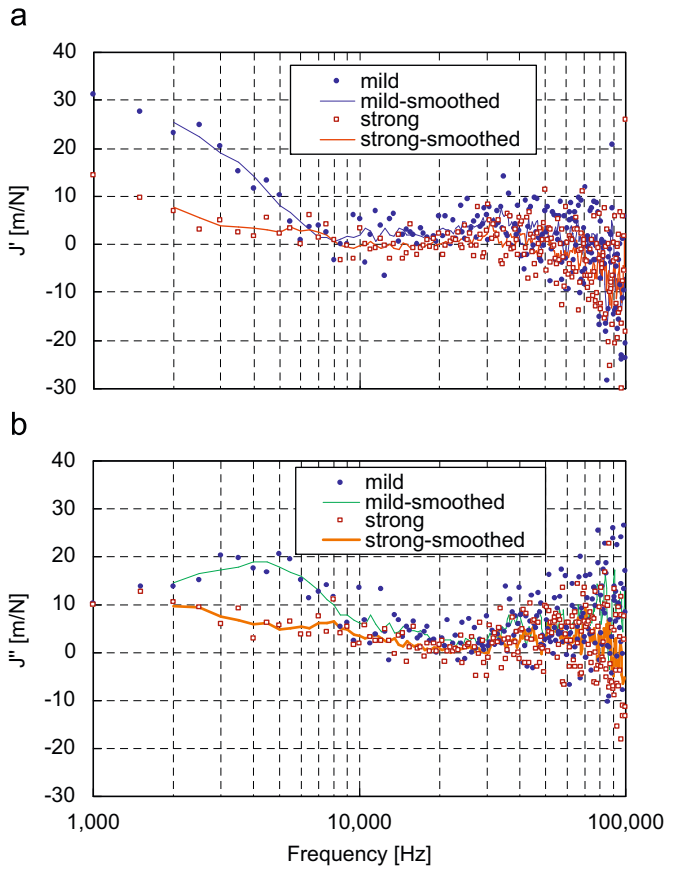

Fig. 7. Comparison of mild and strong interactions with the mica substrate in real (a) and imaginary (b) parts of compliance derived from the data shown in Fig. 6. Data of mild and strong interactions are shown in filled and open figures, respectively. Results of smoothing by taking moving average of 5 data points are also indicated in fine and broad lines for mild and strong interactions, respectively.

present work the measured compliance has been discussed in terms of a combined one for the cantilever and the water. A compliance is inverted to the elasticity $K(i\omega)=K'(\omega)+iK''(\omega)$ as

$$K'(\omega)+iK''(\omega)=(J'(\omega)-iJ''(\omega))^{-1}=\frac{J'(\omega)+iJ''(\omega)}{J'(\omega)^2+J''(\omega)^2}. \quad (3)$$

Because elasticities of parallel mechanical elements are additive, it is logically possible to derive change in viscoelasticity of water only by taking difference between the "mild" and "strong" data. Actually, however, the nearly zero values of J' and J'' around 20 kHz mimic a false peak at this frequency in the calculated elasticity and make the subsequent discussion senseless.

5. Conclusion

Because an AFM cantilever is an object of a huge dimension compared to the tip-substrate gap, a macroscopic hydrodynamic effect [16,31] is inevitably superimposed onto the measured viscoelasticity. Frequency-resolved analysis might provide an option to discriminate the truly microscopic structuring effect out of macroscopic squeezing, if they have different characteristic time scales. In order to do so, however, several experimental conditions have to be reexamined to improve quality of the data and the analysis.

In the data shown in Figs. 5 and 7(b), J'' exhibits a mild peaking around 4 kHz, which is attributed to inappropriate Q suppression as mentioned above. In the present work, the Q-control system has to be optimized so that multiple resonance modes are suppressed at the same time. Actually this is not an easy task since the sensitivity to the higher eigenmode deflection varies with mode number and laser spot position in the optical beam deflection method [32], and the equivalent stiffness of the higher eigenmodes are much larger than that of the fundamental mode [33]. Inserting filters in the Q-control loop to separate each mode and setting different optimum gains to it will cause unexpected phase lags and is not helpful. One realistic option is to set the Q-control gain optimum for each resonance mode to secure the data around that frequency and combine the results tuned for different eigenmodes.

Improvement in S/N ratio is also crucial especially for analysis in the higher frequency regime. Although the step response data presented here were averaged for 128 times, increasing the average number implies a longer acquisition time and is not a good option. It will be advantageous to employ a cantilever with a larger spring constant to suppress the Brownian noise. With the stiffer cantilever a measurement with a deflection amplitude smaller than the present value will be possible, which will open up a path to a more microscopic analysis. In addition, since eigenmode frequencies of a stiff cantilever are generally expected to be higher than those of the present soft cantilever, it will be advantageous in extending the analysis bandwidth, which is limited by the lowest surviving eigenmode of the cantilever.

The effective frequency range of the present analysis scheme is considered to be below 1 MHz at most. Among various soft-matter systems, polymers exhibit characteristic viscoelastic behavior in this frequency range. This method might be useful in probing viscoelastic response of locally inhomogeneous polymers like phase-separated ones or polymer thin films. In addition, with this setup it will be also possible to measure relaxation response of a single polymer chain tethered between the tip and the substrate.

References

[1] E.-L. Florin, V.T. Moy, H.E. Gaub, Science 264 (1994) 415.
[2] U. Dammer, O. Popescu, P. Wagner, D. Anselmetti, H.-J. Giintherodt, G.N. Misevic, Science 267 (1995) 1173.
[3] K. Mitsui, M. Hara, A. Ikai, FEBS Lett. 385 (1996) 29.
[4] A.D.L. Humphris, J. Tamayo, M.J. Miles, Langmuir 16 (2000) 7891.
[5] M. Kageshima, S. Takeda, A. Ptak, C. Nakamura, S.P. Jarvis, H. Tokumoto, J. Miyake, Jpn. J. Appl. Phys. 43 (2004) L1510.
[6] M. Kawakami, K. Byrne, T.C.B. Bhavin Khatri, S.E. Mcleish, Radford, D.A. Smith, Langmuir 20 (2004) 9299.
[7] M. Kawakami, K. Byrne, T.C.B. Bhavin Khatri, S.E. Mcleish, Radford, D.A. Smith, Langmuir 21 (2005) 4765.
[8] H. Janovjak, D.J. Müller, A.D.L. Humphris, Biophys. J. 88 (2005) 1423.
[9] M. Kawakami, K. Byrne, D.J. Brockwell, S.E. Radford, D.A. Smith, Biophys. J. 91 (2006) L16.
[10] M. Kageshima, Y. Nishihara, Y. Hirata, T. Inoue, Y. Naitoh, Y. Sugawara, AIP Conf. Proc. 982 (2008) 504.
[11] M. Kageshima, T. Chikamoto, T. Ogawa, Y. Hirata, T. Inoue, Y. Naitoh, Y.J. Li, Y. Sugawara, Rev. Sci. Instrum. 80 (2009) 023705.
[12] S. Jeffery, P.M. Hoffmann, J.B. Pethica, C. Ramanujan, H. Özer, A. Oral, Phys. Rev. B 70 (2004) 054114.
[13] A. Maali, T. Cohen-Bouhacina, G. Couturier, J.-P. Aimé, Phys. Rev. Lett. 96 (2006) 086105.
[14] T.-D. Li, E. Riedo, Phys. Rev. Lett. 100 (2008) 106102.
[15] S. Hiratsuka, Y. Mizutani, M. Tsuchiya, K. Kawahara, H. Tokumoto, T. Okajima, Ultramicroscopy 109 (2009) 937.
[16] F. Beumouna, D. Johannsmann, Eur. Phys. J. E 9 (2002) 435.
[17] S.P. Jarvis, A. Oral, T.P. Weihs, J.B. Pethica, Rev. Sci. Instrum. 64 (1993) 3515.
[18] E.-L. Florin, M. Radmacher, B. Fleck, H.E. Gaub, Rev. Sci. Instrum. 65 (1994) 639.
[19] S.J. O'Shea, M.E. Welland, T. Rayment, Appl. Phys. Lett. 60 (1992) 2356.
[20] J.P. Cleveland, T.E. Schäffer, P.K. Hansma, Phys. Rev. B 52 (1995) R8692.
[21] S.P. Jarvis, T. Uchihashi, T. Ishida, H. Tokumoto, Y. Nakayama, J. Phys. Chem. B 104 (2000) 6091.
[22] T. Uchihashi, M. Higgins, Y. Nakayama, J.E. Sader, S.P. Jarvis, Nanotechnology 16 (2005) S49.
[23] L.T. Lim, A.T.S. Wee, S.J. O'Shea, J. Chem. Phys. 130 (2009) 134703.
[24] M. Antognozzi, A.D.L. Humphris, M.J. Miles, Appl. Phys. Lett. 78 (2001) 300.
[25] D. Eisenberg, W. Kauzmann, in: The Structure and Properties of Water, Oxford University Press, London, 1969 For example.

[26] S.R. Kabir, K. Yokoyama, K. Mihashi, T. Kodama, M. Suzuki, Biophys. J. 85 (2003) 3154.
[27] H.S. Green, The molecular theory of fluids (North-Holland, Amsterdam, 1952), and references therein.
[28] E.N. da, C. Andrade, Phil. Mag. 17 (1934) 497;
[] E.N. da, C. Andrade, ibid 17 (1934) 698.
[29] R. Kubo, M. Toda, N. Hashitsume, in: Statistical Physics II: Nonequilibrium Statistical Mechanics, Springer-Verlag, Berlin, 1985 For example.
[30] J. Mertz, O. Marti, J. Mlynek, Appl. Phys. Lett. 62 (1993) 2344.
[31] A. Roters, D. Johannsmann, J. Phys.: Condens. Matter 8 (1996) 7561.
[32] T.E. Schäffer, H. Fuchs, J. Appl. Phys. 97 (2005) 083524.
[33] J. Melcher, S. Hu, A. Raman, Appl. Phys. Lett. 91 (2007) 053101.